HHS Public Access

Author manuscript

Nat Commun. Author manuscript; available in PMC 2016 February 14.

Published in final edited form as:

Nat Commun. ; 6: 8005. doi:10.1038/ncomms9005.

A Short N-terminal Domain of HDAC4 Preserves Photoreceptors and Restores Visual Function in Retinitis Pigmentosa

Xinzheng Guo[1], **Shao-Bin Wang**[1], **Hongping Xu**[2], **Adema Ribic**[3], **Ethan J. Mohns**[2], **Yu Zhou**[4,5], **Xianjun Zhu**[4,5], **Thomas Biederer**[3], **Michael C. Crair**[2], and **Bo Chen**[1,2,†]

[1]Department of Ophthalmology and Visual Science, Yale University School of Medicine, 300 George Street, Suite 8100, New Haven, CT 06511, USA

[2]Department of Neurobiology, Yale University School of Medicine, 333 Cedar Street, SHM B301, New Haven, CT 06510, USA

[3]Department of Neuroscience, Tufts University School of Medicine, Boston, MA 02111, USA

[4]Sichuan Provincial Key Laboratory for Human Disease Gene Study and Institute of Laboratory Medicine, Sichuan Academy of Medical Sciences and Sichuan Provincial People's Hospital, Chengdu, Sichuan 610072, China

[5]Hospital of University of Electronic Science and Technology of China (UESTC) & Sichuan Provincial People's Hospital, Chengdu, Sichuan 610072, China

Abstract

Retinitis pigmentosa is a leading cause of inherited blindness, with no effective treatment currently available. Mutations primarily in genes expressed in rod photoreceptors lead to early rod death, followed by a slower phase of cone photoreceptor death. Rd1 mice provide an invaluable animal model to evaluate therapies for the disease. We previously reported that overexpression of histone deacetylase 4 (HDAC4) prolongs rod survival in rd1 mice. Here we report a key role of a short N-terminal domain of HDAC4 in photoreceptor protection. Expression of this domain suppresses multiple cell death pathways in photoreceptor degeneration, and preserves even more rd1 rods than the full length HDAC4 protein. Expression of a short N-terminal domain of HDAC4 in transgenic mice carrying the rd1 mutation also prolongs the survival of cone photoreceptors, and partially restores visual function. Our results may facilitate the design of a small protein therapy for some forms of retinitis pigmentosa.

†To whom correspondence should be addressed. b.chen@yale.edu.

Author contributions

B.C. and X.G. designed the experiments; X.G., B.C., S.-B.W., H.X., A.R., E.J.M., Y.Z., and X.Z. performed the experiments and analyzed the data; B.C. supervised the research and co-wrote the manuscript with X.G., T.B., and M.C.C.

Competing financial interests: The authors declare no competing financial interests.

Introduction

Rod and cone photoreceptors of the vertebrate eye are the primary sensory neurons that initiate vision. Many different mutations directly affect these cells, leading to loss of function and degeneration. One such group of diseases, retinitis pigmentosa (RP), is caused by mutations primarily in rod-specific genes [1]. The disease process is initiated in rods, which detect signals in dim light and provide night vision. RP thus first presents as loss of night vision. Unfortunately, cones, which carry out daylight and color vision, also eventually become dysfunctional in RP patients and die, secondary to rod death. Rd1 mice, one of the most commonly used animal models of RP, carry a mutation in the rod-specific gene *PDE6β* (phosphodiesterase 6β subunit), which is also mutated in a subset of RP patients [2, 3, 4]. The rd1 mutation causes rapid and early rod death, followed by cone death, providing an excellent model for human RP. Several therapeutic strategies have been shown to delay photoreceptor death in rd1 mice, with treatments including neurotrophic factors [5], calcium channel blockers [6], antioxidants [7], or anti-apoptosis gene transfer [8]. Histone deacetylase 4 (HDAC4) plays an essential role in supporting the survival of cortical neurons, cerebellar neurons, and retinal neurons [9, 10, 11]. Altered HDAC4 regulation has been linked to a number of neurodegenerative disorders, such as Parkinson's disease [12, 13, 14] and ataxia [15, 16]. We previously reported that overexpression of HDAC4 in rd1 mice prolongs rod photoreceptor survival [11]. As HDAC4 is a relatively large protein with a deacetylase domain and multiple other domains that interact with transcription factors and cofactors [17, 18, 19], as well as other HDACs, we conducted a structure-function analysis to determine the essential domain(s) required to promote rod survival. Surprisingly, a short amino terminal domain, devoid of the majority of the defined functional domains of HDAC4, was able to prolong rod survival. This domain is glutamine-rich and saved even more rods than full-length HDAC4. The greater rod protection efficiency of the N-terminal domain of HDAC4 at least partly involved greater protein stability. HDAC4 functions in the cytoplasm to suppress multiple pathways involved in photoreceptor death. Rods preserved by HDAC4 in rd1 mice are unlikely to function due to the mutation in PDE6β, an essential gene in rod phototransduction. RP patients maintain functional vision for a long period of time after rod degeneration by relying on the remaining function of cones, which are genetically normal. Therefore, saving cones is key to preserving vision in RP. Significantly, expressing a short N-terminal domain of HDAC4 as a transgene in rd1 mice also prolonged the survival of cones, and as a result, partially restored visual function.

Results

A short N-terminal domain of HDAC4 is sufficient for rod protection in rd1 mice

The deacetylase domain of HDAC4 resides in the C-terminal portion of the protein. As a member of Class IIa HDACs, the enzymatic activity of HDAC4 is evolutionarily weak, about 1000-fold less active than Class I HDACs on standard substrates [20]. In cultured cortical neurons, reduction in HDAC4 expression results in loss of all types of neurons without affecting the survival of astrocytes, and the HDAC4 C-terminal catalytic domain is dispensable for neuroprotection [9]. HDAC4 overexpression also protects cultured cerebellar granule cells from low potassium-induced apoptosis [10]. In order to determine the minimal

domain(s) required for rod survival, several deletions of HDAC4 (Fig. 1a) were tested in rd1 mice of the FVB strain background. Deletion alleles were constructed in a plasmid using the broadly active CAG promoter and were tested by electroporation *in vivo* into the subretinal space of rd1 mice at P0. In addition to the HDAC4 plasmid, a CAG-GFP plasmid was included, to mark electroporated cells, along with a Rho-DsRed reporter plasmid that uses the rhodopsin cis-regulatory element to drive expression of DsRed, and thereby mark rod photoreceptors [21]. In rd1 mice, rods die rapidly, with nearly complete rod death by postnatal day 36 (P36) [2, 4, 7, 22]. The survival of rods was assessed at P50 on retinal flat mounts by examination of Rho-DsRed positive cells in areas that were well marked by GFP expression. Overexpression of HDAC4 preserved many DsRed expressing rods, which were also positive for anti-rhodopsin immunoreactivity (Fig. 1b). We quantified the overlap between GFP, DsRed, and the native marker for rods (Supplementary fig. 1). About 98.2% Rho-DsRed positive cells were positive for anti-rhodopsin immunoreactivity, indicating that the Rho-DsRed reporter faithfully labels native rods. And nearly all (99.8%) of Rho-DsRed positive cells were also positive for GFP, indicating high co-transfection efficiency by *in vivo* electroporation. The protection effect was not due to the experimental procedure *per se*, as overexpressing GFP alone did not preserve rods (Fig. 1b control). Remarkably, overexpression of residues 1-747 of the N-terminal portion of HDAC4, which lacks the deacetylase domain [10], preserved many more rods than the full-length HDAC4. By contrast, overexpression of residues 612-1084 of the C-terminal catalytic domain of HDAC4 [17] had no protective effect (Fig. 1c), indicating that the catalytic domain is dispensable for rod survival through HDAC4 overexpression.

The N-terminal portion of HDAC4 interacts with several proteins that may mediate its pro-survival effect in rd1 rods, including the neuronal survival factor MEF2 [15, 23]. Interestingly, a short HDAC4 N-terminal domain incapable of interacting with MEF2, residues 1-129, carries a prominent glutamine-rich region that folds into an α-helix structure [24]. Overexpression of this short N-terminal domain (residues 1-129) of HDAC4 produced a rod-protection effect as robust as HDAC4 residues 1-747 (Fig. 1c). In addition, we inadvertently made an HDAC4 construct, which we term HDAC4*. This construct exhibited even greater efficiency in saving rd1 rods than the full-length HDAC4 protein or HDAC4 residues 1-129 (Fig. 1c). DNA sequencing of HDAC4* revealed a premature stop codon due to the insertion of a repeated sequence (Supplementary fig. 2a). Translation of the HDAC4* sequence predictably produces a protein of 251 residues containing HDAC4 residues 1-126 with an extension of 125 residues translated from the repeated sequence (Supplementary fig. 2b). To verify the protein identity of HDAC4*, we performed a mass spectrometry assay of immunopurified HDAC4* from transfected HEK293T cells with an antibody raised against the N-terminal amino acids 1-19 of HDAC4 (Supplementary fig. 2c). Peptides identified by mass spectrometry confirmed the predicted protein sequence of HDAC4* (Supplementary fig. 2d). Overexpression of the repeated sequence itself, HDAC4* residues 108-251 (Supplementary fig. 2e), did not save rd1 rods (Supplementary fig. 2f). The number of rods preserved by HDAC4 deletion alleles was quantified per 25600 μm^2 in the electroporated areas labeled by co-electroporated CAG-GFP on retinal flat mounts (Fig. 1d). While HDAC4 Full Length saved 24.1 ± 3.6 (mean ± SD, n=5) rods, the number of rods preserved by HDAC4 residues 1-747 (55.8 ± 6.6, n=8) or HDAC4 residues 1-129 (61.4 ± 6.8, n=6)

was significantly greater, and HDAC4* exhibited by far the greatest efficiency in saving rd1 rods (105.5 ± 12.9, n=6).

N-terminal constructs exhibit greater stability than full length HDAC4

To elucidate the differential protective effects evident in HDAC4 deletion alleles, we assayed HDAC4 protein levels using anti-HDAC4 immunohistochemistry at P12, when most rods still remain in rd1 mice. HDAC4 immunoreactivity for the N-terminal alleles was significantly higher than that observed for the full length HDAC4 in the transfected areas labeled by co-electroporated CAG-GFP (Fig. 2a). Normalized HDAC4 immunoreactivity for the various HDAC4 N-terminal constructs (Fig. 2b), and elevated protein levels relative to the full-length HDAC4 (Fig. 2c, d in electroporated retinas correlated positively with their efficiencies in saving rd1 rods. The expression of endogenous HDAC4 was not detected in rd1 retinas at P12 (Fig. 2c and Discussion). The higher protein levels of HDAC4 N-terminal alleles were not due to differences in mRNA levels as measured by quantitative PCR (Fig. 2e).

HDAC4 protein is unstable as it is subjected to caspase-dependent cleavage [25, 26], as well as polyubiquitination and proteasome degradation [27]. This raised the possibility that the greater protective effects observed for the HDAC4 N-terminal alleles might be due to their increased protein stability. To examine the stability of HDAC4 proteins, we expressed full-length HDAC4 or HDAC4 N-terminal alleles in transfected HEK293T cells and measured protein levels using western blots. The decay in protein was monitored over time following treatment with a protein synthesis inhibitor, cycloheximide, initiated at 20 hours post-transfection (Fig. 3a, b). Full-length HDAC4 protein was degraded fairly rapidly, as only ~20% of the protein remained 6 hours after cycloheximide treatment. The endogenous expression of HDAC4 was not detected in 293T cells transfected with GFP or empty vector controls (Supplementary fig. 3). By contrast, residues 1-129 and residues 1-747 of HDAC4 were more stable, with ~75% of the protein detected under the same conditions. HDAC4* was the most stable allele with barely detectable protein degradation when protein synthesis was blocked during the 6 hour time frame. The increased protein stability of the various HDAC4 alleles (Fig. 3b) correlated positively with their greater abundance after electroporation (Fig. 2b, d), and their ability to preserve rods from degeneration in rd1 mice (Fig. 1d).

Phosphorylation of HDAC4 at Ser^{298} and Ser^{302} promotes polyubiquitination and proteasome degradation. The HDAC4-S298A/S302A mutant has Ser^{298} and Ser^{302} mutated to Ala, which mimics the dephosphorylated state of the protein and is therefore more stable than wild type HDAC4 [27]. Indeed, HDAC4-S298A/S302A was more stable, as it decayed more slowly than the wild type HDAC4 protein in the presence of cycloheximide (Fig. 3c, d). To directly test the role of HDAC4 protein stability on rod survival, we examined whether HDAC4-S298A/S302A might lead to increased rod protection using *in vivo* electroporation in rd1 retinas at P0. Quantification of rod survival at P50 showed significantly more rods in HDAC4-S298A/S30 treated retinas (39.4 ± 5.9 rods per 25600 μm^2, mean ± SD, n=3) than with wild type HDAC4 (24.5 ± 3.4 rods per 25600 μm^2, mean ± SD, n=3; Fig. 3e, f). These results suggest that increased HDAC4 protein stability

contributes to greater rod protection, presumably due to persistently higher levels of functional HDAC4 protein.

Requirement of conserved glutamine residues for rod protection

Glutamine-rich sequences have been implicated primarily in pathological roles in neurodegeneration, causing polyglutamine toxicity in Huntington's disease and the formation of amyloid fibrils in Alzheimer's disease [28, 29]. To elucidate the physiological role of the glutamine-rich region of HDAC4, we examined the rod protection efficacy of HDAC4 1-129 19QA and HDAC4 1-129 7QA alleles, which had either 19 glutamines or the 7 most conserved glutamines mutated to alanines (Fig. 4a). HDAC4 residues 1-129 preserved many rods in rd1 mice at P50 following *in vivo* electroporation at P0, while mutation of either all 19 or the 7 most conserved glutamines completely abolished the rod protection effect (Fig. 4b, c). The loss of rod protection in the glutamine to alanine mutants was not due to reduced protein levels, as they were detected at a level comparable to HDAC4 residues 1-129, measured by western blots in transfected HEK293T cells (Fig. 4d). Our results indicate that the conserved glutamine residues are essential for HDAC4-mediated rod protection in rd1 mice. CtBP/RIBEYE, a synaptic protein expressed in rods [30], binds to a conserved P-X-D-L-S/R motif located in the glutamine-rich region of HDAC4 [31]. However, a mutant (HDAC4 1-129 M4, Fig. 4a), defective in CtBP binding [31], preserved as many rd1 rods as HDAC4 residues 1-129 (Fig. 4b, c), suggesting that the rod protection effect of HDAC4 does not involve its interaction with CtBP.

HDAC5, another member of Class IIa HDACs, is highly homologous to HDAC4 in protein sequence and structure [32]. We tested the efficacy of HDAC5 residues 1-160, which contain a glutamine-rich region in its N-terminus, in saving rd1 rods by *in vivo* electroporation. Like HDAC4, many more rods were preserved by the short N-terminal region of HDAC5 (Supplementary fig. 4a, b) in comparison to the full-length HDAC5. The rod protection effect mediated by HDAC4 or HDAC5 was not due to the overexpression of a random low-molecular-weight protein, as electroporation of Histone H3.1, a small protein of high stability expressed in the brain [33], failed to preserve rd1 rods under the same conditions (Supplementary fig. 4a, b).

HDAC4 suppresses multiple photoreceptor cell death pathways in rd1 mice

Multiple pathways may be involved in photoreceptor death in rd1 mice, including disrupted calcium homeostasis, excessive ER (endoplasmic reticulum) stress, increased reactive oxygen species (ROS), aberrant cell cycle progression, and overactivation of Calpain and Parp [34, 35, 36, 37]. To investigate whether HDAC4 interacts with any of these pathways for rod protection, we used quantitative PCR to examine the mRNA expression profile of genes involved in photoreceptor death in rd1 mice at P12, when most photoreceptors remain. In comparison to GFP-electroporated rd1 retinas as a control, the expression of HDAC4*, the most effective form of HDAC4 in saving rd1 rods (Fig. 1d), did not significantly change the mRNA levels for photoreceptor-specific genes (Fig. 5a). We then categorized genes involved in photoreceptor death into 3 groups: transcription factors and cell cycle genes, genes involved in ER stress or oxidative stress, and cell death/apoptosis genes. Genes

upregulated in rd1 retina relative to wild type retina were indicated by a fold change of >1 (dashed lines in Fig. 5b–d).

Gene category 1: transcription factors and cell cycle genes (Fig. 5b). Transcription factors c-fos, c-jun, and p53 are closely associated with retinal degeneration [38, 39]. The mRNA levels for the three genes were strongly upregulated in the rd1 retina, however, HDAC4* had no effect on their expression in the rd1 retina. Cell cycle reactivation is a common feature of neuronal apoptosis during development and in neurodegenerative diseases [40]. Aberrant cell cycle progression was also proposed to be a cause of photoreceptor degeneration in rd1 mice [41]. Two cell cycle genes, *Ccnb1* and *Ccnd1*, were upregulated in the rd1 retina, and HDAC4* treatment significantly reduced the upregulation of both Ccnb1 and Ccnd1.

Gene category 2: ER stress and oxidative stress genes (Fig. 5c). Activation of ER stress genes, including Atf4, Bip, Chop, and Caspase-12, is implicated in degenerating photoreceptors in rd1 mice [42]. Similarly, genes involved in oxidative stress, including *Aop2*, *Gstm1*, and *Ogg1*, are also activated during photoreceptor degeneration [43, 44]. Similarly, upregulation of *ASK1* can be triggered by both ER stress and oxidative stress [45]. Consistent with previous findings, significant upregulation of this gene category was detected in the control GFP-treated rd1 mice. Noticeably, HDAC4* treatment attenuated the upregulation of these stress genes, especially the level of Chop expression.

Gene category 3: cell death/apoptosis genes (Fig. 5d). The Bcl-2 family, which contains both pro-apoptotic (*Bad*, *Bax*, and *Bid*) and anti-apoptotic (*Bcl2*) genes, regulates the mitochondrial pathway of apoptosis by controlling the permeabilization of the outer mitochondrial membrane. The ratio of the two subsets determines the susceptibility of cells to cell death signals [46]. Significantly, the upregulation of the pro-apoptotic gene *Bid* was reduced by HDAC4* treatment. Calpain is a group of calcium-dependent cysteine proteases with substrates that include proteins regulating apoptosis such as PARP and AIF. Calpain is strongly activated in degenerating rd1 photoreceptors in rd1 mice [47]. PARP, poly (ADP-ribose) polymerase, an enzyme involved in DNA repair, is excessively activated in rd1 mice leading to caspase-independent cell death [48, 49]. HDAC4* treatment attenuated the upregulation of both Calpain2 and Parp1.

Our results indicate that HDAC4* treatment suppressed multiple cell death pathways involved in photoreceptor degeneration in rd1 mice. To determine whether the endogenous HDAC4 is required for HDAC4*-mediated rod survival in rd1 mice, we utilized a plasmid containing a short hairpin RNA (shRNA) to knock down the expression of the native HDAC4 while co-electroporating an allele of HDAC4* resistant to the shRNA [11]. No significant reduction was seen in the number of preserved rd1 rods at P50 when endogenous HDAC4 expression was knocked down (Supplementary fig. 5). HDAC4 shuttles between the nucleus and cytoplasm [50, 51]. It functions as a transcriptional repressor to regulate bone and muscle differentiation in the nucleus [17, 18, 52, 53]. To investigate whether HDAC4 exerted its rod protection effect by engaging in activities in the nucleus or cytoplasm, we examined the localization of electroporated HDAC4 alleles in rd1 mice at P12 using fluorescence confocal microscopy. In addition to the cytoplasmic distribution, the co-electroporated GFP was also observed in the nucleus revealing the typical heterochromatin

structure of rods. In comparison to the GFP localization, the full-length HDAC4 and HDAC4 N-terminal deletion alleles were mainly seen in the cytoplasm of the electroporated rods (Supplementary fig. 6). Our results indicate that HDAC4 functions in the cytoplasm to protect rd1 rods.

HDAC4 acts in a cell-autonomous manner to protect rd1 rods

Many non-photoreceptor cells, including bipolar cells, Müller glial cells, and amacrine cells, are transfected by *in vivo* electroporation. To distinguish whether HDAC4 preserved rd1 rods through a cell-autonomous process or indirectly due to its expression in other cell types, we utilized a Cre-recombinase responsive expression system for cell-type-specific expression of HDAC4* (Fig. 6a) with a plasmid containing a ubiquitous CAG promoter and a floxed “stop cassette”. Rod-specific expression of HDAC4 was achieved by co-electroporation of Rho-Cre, a Cre-expression plasmid driven by the rhodopsin promoter [21, 54]. Rods (83.2 ± 10.7, n=3) were preserved in rd1 mice at P50 only in the presence of Rho-Cre (Fig. 6b, c). As the rhodopsin promoter becomes active when rod precursors differentiate to mature rods [54], our results suggest that HDAC4 can be introduced at late postnatal stages to preserve rd1 rods in a cell-autonomous manner.

HDAC4* saves cone photoreceptors, and restores visual function

Electroporation in the neonatal mouse retina results in transfection of many rods, but few cones [21]. Rd1 rods preserved by HDAC4 are unlikely to function due to the mutation in the rod-specific gene *PDE6β*, which encodes a key enzyme in the rod phototransduction cascade. Rods mediate vision in dim light, whereas cones are responsible for day light vision and visual acuity. RP patients maintain functional vision after rod degeneration for a long period of time due to the remaining function of cones, which are genetically normal. To investigate whether HDAC4 gene transfer saves cones as well as rods, and as a result, may restore visual function, we generated transgenic mice that express HDAC4* in FVB mice (a mouse strain homozygous for the rd1 mutation). HDAC4* expression was driven by a broadly active promoter, CAG, generating a photoreceptor-dominant expression pattern in a transgenic context [55]. An IRES (internal ribosome entry site) sequence was included in the transgenic construct (Fig. 7a) to simultaneously express GFP as a reporter for the HDAC4* transgene expression. We assayed transgene expression using western blots at P10, when most photoreceptors remain. While the endogenous HDAC4 was detected at a comparable expression level in HDAC4* transgenic mice and their non-transgenic littermates, HDAC4* and GFP were only detected in the HDAC4* transgenic mice, with HDAC4* expressed at a level about 3 times that of endogenous HDAC4 (Fig. 7b). We next examined transgene expression by anti-HDAC4 immunohistochemistry or GFP fluorescence in P10 retinal sections (Fig. 7c). HDAC4 immunoreactivity and GFP were detected predominantly in the perinuclear space of the outer nuclear layer (ONL) of photoreceptors and the outer and inner segments of photoreceptors (Fig. 7d). Transgene expression, indicated by the GFP reporter, was evident in both rods labeled by anti-rhodopsin immunoreactivity (Fig. 7e), and cones labeled by anti-red/green cone opsin immunoreactivity (Fig. 7f). Transgene expression was also weakly detected in a subset of other cell types in the inner nuclear layer (INL) (Supplementary fig. 7).

Photoreceptor degeneration starts in the center and propagates to the periphery in rd1 mice [4]. We examined rod and cone photoreceptor survival at P42 in HDAC4* transgenic mice in comparison to their non-transgenic littermates by counting anti-rhodopsin immunoreactive cells or peanut agglutinin (PNA, a cone marker) labeled cells in four retinal quadrants (dorsal, ventral, temporal, and nasal) at two distances (700μm and 1400μm) from the center of the retina (Supplementary fig. 8). For rod survival at 700μm from the center of the retina (Fig. 8a, b), fewer than 10 rods remained in each of the 4 quadrants from non-transgenic littermates, while more than 100 rods were scored in corresponding areas in HDAC4* transgenic mice (n=8). At 1400 μm from the center of the retina (Fig. 8c, d), 25–50 rods remained in the non-transgenic littermates compared to 180–250 scored rods in the HDAC4* transgenic mice (n=8). For cone survival at 700μm (Fig. 9a, b) or 1400 μm (Fig 9c, d) from the center of the retina, HDAC4* expression significantly increased cone density in all four quadrants of the retina in HDAC4* transgenic mice compared to their non-transgenic littermates (n=8).

We examined whether HDAC4-mediated photoreceptor protection leads to improved visual function by recording electroretinograms (ERGs) in HDAC4* transgenic mice in comparison to their non-transgenic littermates in the same FVB strain background at P30. Scotopic ERG recordings were performed in dark-adapted animals with increasing light intensities from −3.6 to 2.9 log cd.s/m^2. In wild type mice, dim light flashes between −4.0 to −2.0 log cd.s/m^2 elicit responses from rods while cones start to be activated by brighter light stimuli [56, 57]. Compared to typical ERG responses recorded from C57BL/6 wild type mice (Fig. 10a), no ERG response was detected in either dim or higher light intensities from non-transgenic rd1 mice (Fig. 10b). In HDAC4* transgenic mice, no significant ERG response was elicited in lower light intensities until the light intensity increased to 1.4 log cd.s/m^2 (Fig. 10c, d), indicating recovered function from cones. We further introduced the expression of a wild type allele of *PDE6β* by *in vivo* electroporation in HDAC4* transgenic mice. The ERG recordings still showed no improved rod function in the *PDE6β*-electroporated HDAC4* transgenic mice (Supplementary fig. 9). The lack of recovery in rod function might be due to a limited number of PDE6β-transfected rods that appear in small patches typically generated by electroporation, resulting in undetectable responses by whole-field ERG recordings. We next recorded photopic ERGs to measure cone function in light-adapted animals. While photopic ERG responses were hardly detectable in the non-transgenic rd1 littermates, HDAC4* transgenic mice showed a noticeable photopic ERG response (Fig. 10e) with a significant b-wave amplitude (38.3 ± 6.31 μV, n=11) (Fig. 10f). These results indicate that HDAC4* gene transfer in photoreceptors can partially restore cone-mediated visual function in rd1 mice.

Discussion

HDAC4 is a relatively large protein with many domains and a somewhat weak deacetylase domain [20]. It is shown to bind to several transcription factors and thereby play roles in muscle and bone development [17, 18, 52, 58]. It also binds to Class I HDACs, such as HDAC1 and HDAC3 [19, 59]. Here we show that none of these domains are required for the survival-promoting activity of HDAC4 in degenerating retinas. Surprisingly, a very short amino terminal domain with high glutamine content had as much rod protection function as the full

length HDAC4. In addition, an allele with some repeated elements from HDAC4, appended to the short glutamine-rich region, provided even greater protection. The basis of the differential rod protection effect is likely protein stability, which results in higher levels of HDAC4. Identification of the minimum functional domain of HDAC4 required for photoreceptor protection will likely aid in the design of a small protein therapeutic intervention for retinal degenerative diseases.

HDAC4 is a dynamic protein with a regulated short half-life under normal conditions. The stability of HDAC4 is regulated by caspase-mediated cleavage at Asp-289 as the prime cleavage site [25] and polyubiquitination-proteasome degradation triggered by phosphorylation at Ser-298 and Ser-302 [60]. We found that HDAC4 amino terminal alleles preserved more rods, and were more stable, than the HDAC4 full-length protein, establishing a positive correlation between protein stability and rod protection efficiency. The HDAC4-S298A/S302A mutant, which is resistant to ubiquitination-proteasome degradation and is thus more stable, also showed a greater effect in preserving rd1 rods relative to the wild type allele. HDAC4*, the most stable form with high glutamine content, is the most efficient in saving rd1 rods. HDAC4 protein stability may contribute to greater efficiency in promoting photoreceptor survival, possibly due to higher protein levels.

In rd1 mice, massive degeneration of rod photoreceptors starts around P10. Accumulation of cGMP, due to the rd1 mutation in *PDE6β*, is considered the trigger for rod death. While showing common features of apoptosis [61, 62], such as DNA fragmentation, the exact mechanism leading to photoreceptor degeneration remains elusive. Cytochrome c-mediated apoptotic pathway may not play a critical role as its release from mitochondria was not detected in the rd1 retina [63]. Multiple pathways may be implicated in the photoreceptor degeneration. Our results indicate that HDAC4 may interfere with at least several pathways by suppressing the expression of genes that are upregulated in degenerating photoreceptors. Interestingly, the endogenous expression of HDAC4 was significantly downregulated during photoreceptor degeneration in the rd1 retina as we detected it at P10 (Fig. 7b), but were unable to do so at P12 (Fig. 2c). The reduced expression of the endogenous HDAC4 in rd1 mice may have contributed to the fast cell death of rods as HDAC4 is required for the survival of rods and bipolar cells in normal retina [11].

Retinitis pigmentosa can lead to complete blindness, due to dysfunction and then death of both rod and cone photoreceptors, with no effective treatment currently available. Rd1 mice, which exhibit a pathology very similar to that of humans, provide an invaluable animal model for the evaluation of therapies for this disease. RP is genetically heterogeneous, with many of the disease mutations in rod-specific genes, including those essential for rod phototransduction, such as rhodopsin and *PDE6β*. Cones, genetically and functionally normal in many cases of RP, degenerate secondarily to rod death. Several hypotheses have been proposed to explain why normal cones die in RP, which include: the lack of rod-derived trophic factors [64], the release of toxic factors by dying rods [65], the compromised contact-mediated structure between the retina and the retinal pigmented epithelium [66], and poor nutritional support for cones [67]. Saving cones is key to preserving the vision of RP patients. Several approaches have prolonged the survival of cones in rd1 mice. These include treatments with calcium channel blockers [6], antioxidants [7], and the manipulation of

cell cycle regulators [41], all of which have been shown to preserve cone function, as indicated by ERG measurements. We found that HDAC4* prolonged the survival of cones in transgenic mice harboring the rd1 mutation. Significantly, HDAC4*-mediated cone photoreceptor protection generated a photopic ERG response. HDAC4* gene transfer thus may provide a potential treatment for photoreceptor disease by prolonging the survival of photoreceptors. Compared to the fast rod death in rd1 mice, cones are insensitive to light long before they die. Introduction of halorhodopsin, an optogenetic protein, into rd1 cones restored light sensitivity to cones, as well as vision [68]. The combination of HDAC4 and halorhodopsin might provide both greater survival as well as prolonged function in any disease where photoreceptors lose light responses and degenerate.

Methods

Constructs and retinal electroporation

HDAC4 and various HDAC4 deletion alleles were constructed into the pCAGEN vector (Addgene) for *in vivo* electroporation. In short, Newborn rd1 mouse pups (FVB strain) were anesthetized by chilling on ice, and a small incision was made in the eyelid with a 30-gauge needle to expose the eyeball. DNA mix (1μg/μl of each plasmid) was injected into the subretinal space with a Hamilton syringe followed by electroporation with a tweezer-type electrode and the ECM830 (BTX) pulse generator applying five 80 volts square pulses for 50 ms duration each pulse and 950 ms intervals.

Immunoprecipitation and immunoblotting from transfected cells

HEK293T cells (ATCC) were cultured in DMEM (Gibco) with 10% FBS (Sigma) and penicillin-streptomycin (Lonza). Transfection was performed using Lipofectamine 2000 (Life Technologies). For immunopurification, CAG-HDAC4* transfected cells were collected 48 hours post-transfection. Cleared cell lysates were incubated with an anti-HDAC4 antibody raised against residues 1-19 of human HDAC4 (Sigma), and bound proteins were precipitated with Protein A/G plus agarose beads (Santa Cruz Biotechnology). For immunoblotting, retinal tissues or cells were lysed by boiling in 2% SDS Sample Buffer. Proteins were separated by SDS-PAGE and electro-transferred onto PVDF membranes (Bio-Rad). Primary antibody: HDAC4 (Sigma, 1/2000), GFP (Thermo scientific, 1/2000), β-Actin (Thermo Scientific, 1/3000). Secondary antibody: HRP-linked anti-mouse IgG (Cell Signaling, 1/4000). The antigens were detected using Pierce ECL Western Blotting Substrate (Thermo Scientific) and HyBlot CL autoradiography film (Denvilles Scientific). Full scan images of western blots data are provided in Supplementary Figure 10.

Mass spectrometry

In gel protein digestion: The SDS PAGE separated protein band of HDAC4* was excised and washed with acetonitrile/ammonium bicarbonate/acetonitrile buffers. After washing, the gel was speedvaced to dryness, rehydrated with 45μl of 0.0067μg trypsin (Promega), and digested at 37 °C for 16 hours. LC-MS/MS on the LTQ Orbitrap: LC-MS/MS analysis was performed on a Thermo Scientific LTQ Orbitrap equipped with a Waters nanoAcquity UPLC system. Sample trapping was done at 15μl/min, 99% Buffer A (100% water, 0.1% formic acid) for 1 minute on a Waters Symmetry® C18 180μm × 20mm trap column.

Peptide separation was at 300nl/min on a1.7 μm, BEH130 C18, 75 μm × 250 mm nanoAcquity™ UPLC™ column (35°C). A linear gradient was run at initial conditions. MS was acquired in the Orbitrap using 1 microscan, 30,000 resolution and a maximum inject time of 900 followed by six data dependant MS/MS acquisitions in the ion trap. The data was searched using Mascot Distiller and the Mascot search algorithm.

Immunohistochemistry and fluorescence microscopy

Retinas were fixed in 4% paraformaldehyde in PBS for at least 30min at room temperature for retinal flat mount or cryosection. Primary antibodies: HDAC4 (Sigma, 1:200), Rhodopsin (Rho4D2, 1:100), Red/Green opsin (Millipore, 1:200) and biotin-conjugated Peanut agglutinin (PNA) (1:300). Secondary antibodies: DyLight 594/647-conjugated affiniPure antibodies or streptavidin (Jackson ImmunoResearch). Confocal images were acquired using a Zeiss LSM 510 EXCITER microscope. Images were analyzed in Image J.

RNA extraction and quantitative PCR

Total RNAs from electroporated retinas were isolated using TRIzol reagent (Life Technologies) according to manufacturer's instructions. cDNAs were synthesized with the RETROscript kit (Life Technologies) kit and then used as templates for PCR amplification. Real-time PCR was performed using SsoFas EvaGreen supermix (Bio-Rad) reagent with iCycler iQ™ Real-Time PCR Detection System. Primer sequences are listed in Supplementary Table 1.

Generation of HDAC4* transgenic mice and genotyping

All animal experiments were performed in accordance with the animal protocol approved by the Institutional Animal Care and Use Committee of Yale University. Linearized HDAC4* pCAGIG vector (Addgene) was used for FVB mouse zygote pronuclear microinjection (Gene Targeting and Transgenic Facility, University of Connecticut Health Center). Transgenic founders were identified by genotyping with PCR primers: AAACACGATGATAATATGGC and TCATGTGGTCGGGGTAG. Established HDAC4* transgenic lines are maintained by breeding hemizygous males to non-transgenic FVB females. Male and female C57BL/6 mice at 8–10 weeks of age were purchased from The Jackson Laboratory (Bar Harbor, Maine).

ERG recordings

ERGs were recorded using an UTAS visual electrodiagnostic system equipped with BigShot Ganzfeld stimulator (LKC Technologies, Inc.). Mice were anesthetized with a mix of ketamine (100 mg/kg) and xylazine (10 mg/kg) by intraperitoneal injection. Pupils were dilated with 1% tropicamide (Alcon) and 1% Atropine. A pair of platinum electrodes was placed on each cornea, a reference electrode was placed subcutaneously in the anterior scalp between the eyes, and a ground electrode was inserted into the tail. Corneal hydration was maintained by application of Blink Gel Tears lubricating eye drops (Abbott). For scotopic ERG, mice were dark-adapted and stimulated with flashes of increasing light intensity (−3.6, −2.6, −1.6, −0.6, 0.4, 1.4, and 2.9 log cd.s/m^2). For photopic ERG, mice were light-adapted for 15 minutes and stimulated with flashes (2.9 log cd.s/m^2) in the presence of a white

background light (30 cd/m^2). Signals were band-pass filtered between 0.3 Hz to 100 Hz and averaged response from 16 single flashes were recorded and analyzed.

Statistical analysis

Data are presented as mean ± SD. A two-tailed Student's t-test was used to determine the statistical significance between different experimental groups.

Supplementary Material

Refer to Web version on PubMed Central for supplementary material.

Acknowledgments

We thank Dr. Claudio Brancolini for providing HDAC4-S298A/S302A mutant; Kathryn Stone at the Yale Proteomics Resource Laboratory for Mass Spectrometry analysis; Dr. Laura Frishman for advice on ERG recordings; Dr. Constance L. Cepko for scientific discussion and feedback on the manuscript. This research was supported by National Institutes of Health grant R01 EY021502, The Karl Kirchgessner Foundation, and an unrestricted grant from Research to Prevent Blindness to Yale University.

References

1. Berson EL. Retinitis pigmentosa: unfolding its mystery. Proc Natl Acad Sci U S A. 1996; 93:4526–4528. [PubMed: 8643437]
2. McLaughlin ME, Sandberg MA, Berson EL, Dryja TP. Recessive mutations in the gene encoding the beta-subunit of rod phosphodiesterase in patients with retinitis pigmentosa. Nat Genet. 1993; 4:130–134. [PubMed: 8394174]
3. Hartong DT, Berson EL, Dryja TP. Retinitis pigmentosa. Lancet. 2006; 368:1795–1809. [PubMed: 17113430]
4. Carter-Dawson LD, LaVail MM, Sidman RL. Differential effect of the rd mutation on rods and cones in the mouse retina. Invest Ophthalmol Vis Sci. 1978; 17:489–498. [PubMed: 659071]
5. LaVail MM, et al. Protection of mouse photoreceptors by survival factors in retinal degenerations. Invest Ophthalmol Vis Sci. 1998; 39:592–602. [PubMed: 9501871]
6. Frasson M, Sahel JA, Fabre M, Simonutti M, Dreyfus H, Picaud S. Retinitis pigmentosa: rod photoreceptor rescue by a calcium-channel blocker in the rd mouse. Nat Med. 1999; 5:1183–1187. [PubMed: 10502823]
7. Komeima K, Rogers BS, Lu L, Campochiaro PA. Antioxidants reduce cone cell death in a model of retinitis pigmentosa. Proc Natl Acad Sci U S A. 2006; 103:11300–11305. [PubMed: 16849425]
8. Bennett J, Zeng Y, Bajwa R, Klatt L, Li Y, Maguire AM. Adenovirus-mediated delivery of rhodopsin-promoted bcl-2 results in a delay in photoreceptor cell death in the rd/rd mouse. Gene Ther. 1998; 5:1156–1164. [PubMed: 9930315]
9. Sando R 3rd, Gounko N, Pieraut S, Liao L, Yates J 3rd, Maximov A. HDAC4 governs a transcriptional program essential for synaptic plasticity and memory. Cell. 2012; 151:821–834. [PubMed: 23141539]
10. Majdzadeh N, Wang L, Morrison BE, Bassel-Duby R, Olson EN, D'Mello SR. HDAC4 inhibits cell-cycle progression and protects neurons from cell death. Dev Neurobiol. 2008; 68:1076–1092. [PubMed: 18498087]
11. Chen B, Cepko CL. HDAC4 regulates neuronal survival in normal and diseased retinas. Science. 2009; 323:256–259. [PubMed: 19131628]
12. Takahashi-Fujigasaki J, Fujigasaki H. Histone deacetylase (HDAC) 4 involvement in both Lewy and Marinesco bodies. Neuropathol Appl Neurobiol. 2006; 32:562–566. [PubMed: 16972890]
13. Kirsh O, et al. The SUMO E3 ligase RanBP2 promotes modification of the HDAC4 deacetylase. Embo J. 2002; 21:2682–2691. [PubMed: 12032081]

14. Um JW, Min DS, Rhim H, Kim J, Paik SR, Chung KC. Parkin ubiquitinates and promotes the degradation of RanBP2. J Biol Chem. 2006; 281:3595–3603. [PubMed: 16332688]
15. Bolger TA, Zhao X, Cohen TJ, Tsai CC, Yao TP. The neurodegenerative disease protein ataxin-1 antagonizes the neuronal survival function of myocyte enhancer factor-2. J Biol Chem. 2007; 282:29186–29192. [PubMed: 17646162]
16. Li J, et al. Nuclear accumulation of HDAC4 in ATM deficiency promotes neurodegeneration in ataxia telangiectasia. Nat Med. 2012; 18:783–790. [PubMed: 22466704]
17. Miska EA, Karlsson C, Langley E, Nielsen SJ, Pines J, Kouzarides T. HDAC4 deacetylase associates with and represses the MEF2 transcription factor. Embo J. 1999; 18:5099–5107. [PubMed: 10487761]
18. Vega RB, et al. Histone deacetylase 4 controls chondrocyte hypertrophy during skeletogenesis. Cell. 2004; 119:555–566. [PubMed: 15537544]
19. Chan JK, Sun L, Yang XJ, Zhu G, Wu Z. Functional characterization of an amino-terminal region of HDAC4 that possesses MEF2 binding and transcriptional repressive activity. J Biol Chem. 2003; 278:23515–23521. [PubMed: 12709441]
20. Lahm A, et al. Unraveling the hidden catalytic activity of vertebrate class IIa histone deacetylases. Proc Natl Acad Sci U S A. 2007; 104:17335–17340. [PubMed: 17956988]
21. Matsuda T, Cepko CL. Electroporation and RNA interference in the rodent retina in vivo and in vitro. Proc Natl Acad Sci U S A. 2004; 101:16–22. [PubMed: 14603031]
22. Bowes C, Li T, Danciger M, Baxter LC, Applebury ML, Farber DB. Retinal degeneration in the rd mouse is caused by a defect in the beta subunit of rod cGMP-phosphodiesterase. Nature. 1990; 347:677–680. [PubMed: 1977087]
23. Mao Z, Bonni A, Xia F, Nadal-Vicens M, Greenberg ME. Neuronal activity-dependent cell survival mediated by transcription factor MEF2. Science. 1999; 286:785–790. [PubMed: 10531066]
24. Guo L, Han A, Bates DL, Cao J, Chen L. Crystal structure of a conserved N-terminal domain of histone deacetylase 4 reveals functional insights into glutamine-rich domains. Proc Natl Acad Sci U S A. 2007; 104:4297–4302. [PubMed: 17360518]
25. Liu F, Dowling M, Yang XJ, Kao GD. Caspase-mediated specific cleavage of human histone deacetylase 4. J Biol Chem. 2004; 279:34537–34546. [PubMed: 15205465]
26. Paroni G, Mizzau M, Henderson C, Del Sal G, Schneider C, Brancolini C. Caspase-dependent regulation of histone deacetylase 4 nuclear-cytoplasmic shuttling promotes apoptosis. Mol Biol Cell. 2004; 15:2804–2818. [PubMed: 15075374]
27. Cernotta N, Clocchiatti A, Florean C, Brancolini C. Ubiquitin-dependent degradation of HDAC4, a new regulator of random cell motility. Mol Biol Cell. 2011; 22:278–289. [PubMed: 21118993]
28. Perutz MF, Johnson T, Suzuki M, Finch JT. Glutamine repeats as polar zippers: their possible role in inherited neurodegenerative diseases. Proc Natl Acad Sci U S A. 1994; 91:5355–5358. [PubMed: 8202492]
29. Nelson R, et al. Structure of the cross-beta spine of amyloid-like fibrils. Nature. 2005; 435:773–778. [PubMed: 15944695]
30. Schmitz F, Konigstorfer A, Sudhof TC. RIBEYE, a component of synaptic ribbons: a protein's journey through evolution provides insight into synaptic ribbon function. Neuron. 2000; 28:857–872. [PubMed: 11163272]
31. Zhang CL, McKinsey TA, Lu JR, Olson EN. Association of COOH-terminal-binding protein (CtBP) and MEF2-interacting transcription repressor (MITR) contributes to transcriptional repression of the MEF2 transcription factor. J Biol Chem. 2001; 276:35–39. [PubMed: 11022042]
32. Yang XJ, Gregoire S. Class II histone deacetylases: from sequence to function, regulation, and clinical implication. Mol Cell Biol. 2005; 25:2873–2884. [PubMed: 15798178]
33. Toyama BH, et al. Identification of long-lived proteins reveals exceptional stability of essential cellular structures. Cell. 2013; 154:971–982. [PubMed: 23993091]
34. Rohrer B, Pinto FR, Hulse KE, Lohr HR, Zhang L, Almeida JS. Multidestructive pathways triggered in photoreceptor cell death of the rd mouse as determined through gene expression profiling. J Biol Chem. 2004; 279:41903–41910. [PubMed: 15218024]

35. Doonan F, Donovan M, Cotter TG. Activation of multiple pathways during photoreceptor apoptosis in the rd mouse. Invest Ophthalmol Vis Sci. 2005; 46:3530–3538. [PubMed: 16186330]
36. Lohr HR, Kuntchithapautham K, Sharma AK, Rohrer B. Multiple, parallel cellular suicide mechanisms participate in photoreceptor cell death. Exp Eye Res. 2006; 83:380–389. [PubMed: 16626700]
37. Sancho-Pelluz J, et al. Photoreceptor cell death mechanisms in inherited retinal degeneration. Mol Neurobiol. 2008; 38:253–269. [PubMed: 18982459]
38. Hafezi F, et al. The absence of c-fos prevents light-induced apoptotic cell death of photoreceptors in retinal degeneration in vivo. Nat Med. 1997; 3:346–349. [PubMed: 9055866]
39. Ali RR, et al. Absence of p53 delays apoptotic photoreceptor cell death in the rds mouse. Curr Eye Res. 1998; 17:917–923. [PubMed: 9746439]
40. Greene LA, Liu DX, Troy CM, Biswas SC. Cell cycle molecules define a pathway required for neuron death in development and disease. Biochim Biophys Acta. 2007; 1772:392–401. [PubMed: 17229557]
41. Zencak D, et al. Retinal degeneration depends on Bmi1 function and reactivation of cell cycle proteins. Proc Natl Acad Sci U S A. 2013; 110:E593–601. [PubMed: 23359713]
42. Yang LP, Wu LM, Guo XJ, Tso MO. Activation of endoplasmic reticulum stress in degenerating photoreceptors of the rd1 mouse. Invest Ophthalmol Vis Sci. 2007; 48:5191–5198. [PubMed: 17962473]
43. Hackam AS, et al. Identification of gene expression changes associated with the progression of retinal degeneration in the rd1 mouse. Invest Ophthalmol Vis Sci. 2004; 45:2929–2942. [PubMed: 15326104]
44. Cortina MS, Gordon WC, Lukiw WJ, Bazan NG. Oxidative stress-induced retinal damage up-regulates DNA polymerase gamma and 8-oxoguanine-DNA-glycosylase in photoreceptor synaptic mitochondria. Exp Eye Res. 2005; 81:742–750. [PubMed: 15979612]
45. Sekimukai D, Honda S, Negi A. RNA interference for apoptosis signal-regulating kinase-1 (ASK-1) rescues photoreceptor death in the rd1 mouse. Mol Vis. 2009; 15:1764–1773. [PubMed: 19727340]
46. Brunelle JK, Letai A. Control of mitochondrial apoptosis by the Bcl-2 family. J Cell Sci. 2009; 122:437–441. [PubMed: 19193868]
47. Paquet-Durand F, Azadi S, Hauck SM, Ueffing M, van Veen T, Ekstrom P. Calpain is activated in degenerating photoreceptors in the rd1 mouse. J Neurochem. 2006; 96:802–814. [PubMed: 16405498]
48. Sahaboglu A, et al. PARP1 gene knock-out increases resistance to retinal degeneration without affecting retinal function. PLoS One. 2010; 5:e15495. [PubMed: 21124852]
49. Paquet-Durand F, et al. Excessive activation of poly(ADP-ribose) polymerase contributes to inherited photoreceptor degeneration in the retinal degeneration 1 mouse. J Neurosci. 2007; 27:10311–10319. [PubMed: 17881537]
50. Wang AH, Yang XJ. Histone deacetylase 4 possesses intrinsic nuclear import and export signals. Mol Cell Biol. 2001; 21:5992–6005. [PubMed: 11486037]
51. Zhao X, et al. The modular nature of histone deacetylase HDAC4 confers phosphorylation-dependent intracellular trafficking. J Biol Chem. 2001; 276:35042–35048. [PubMed: 11470791]
52. Hoeflich KP, Luo J, Rubie EA, Tsao MS, Jin O, Woodgett JR. Requirement for glycogen synthase kinase-3beta in cell survival and NF-kappaB activation. Nature. 2000; 406:86–90. [PubMed: 10894547]
53. Arnold MA, et al. MEF2C transcription factor controls chondrocyte hypertrophy and bone development. Dev Cell. 2007; 12:377–389. [PubMed: 17336904]
54. Matsuda T, Cepko CL. Controlled expression of transgenes introduced by in vivo electroporation. Proc Natl Acad Sci U S A. 2007; 104:1027–1032. [PubMed: 17209010]
55. Nour M, Quiambao AB, Al-Ubaidi MR, Naash MI. Absence of functional and structural abnormalities associated with expression of EGFP in the retina. Invest Ophthalmol Vis Sci. 2004; 45:15–22. [PubMed: 14691148]
56. Alarcon-Martinez L, et al. ERG changes in albino and pigmented mice after optic nerve transection. Vision Res. 2010; 50:2176–2187. [PubMed: 20727908]

57. Seeliger MW, et al. New views on RPE65 deficiency: the rod system is the source of vision in a mouse model of Leber congenital amaurosis. Nat Genet. 2001; 29:70–74. [PubMed: 11528395]
58. McKinsey TA, Zhang CL, Lu J, Olson EN. Signal-dependent nuclear export of a histone deacetylase regulates muscle differentiation. Nature. 2000; 408:106–111. [PubMed: 11081517]
59. Fischle W, et al. Enzymatic activity associated with class II HDACs is dependent on a multiprotein complex containing HDAC3 and SMRT/N-CoR. Mol Cell. 2002; 9:45–57. [PubMed: 11804585]
60. Cernotta N, Clocchiatti A, Florean C, Brancolini C. Ubiquitin-dependent degradation of HDAC4, a new regulator of random cell motility. Mol Biol Cell. 2011; 22:278–289. [PubMed: 21118993]
61. Chang GQ, Hao Y, Wong F. Apoptosis: final common pathway of photoreceptor death in rd, rds, and rhodopsin mutant mice. Neuron. 1993; 11:595–605. [PubMed: 8398150]
62. Portera-Cailliau C, Sung CH, Nathans J, Adler R. Apoptotic photoreceptor cell death in mouse models of retinitis pigmentosa. Proc Natl Acad Sci U S A. 1994; 91:974–978. [PubMed: 8302876]
63. Doonan F, Donovan M, Cotter TG. Caspase-independent photoreceptor apoptosis in mouse models of retinal degeneration. J Neurosci. 2003; 23:5723–5731. [PubMed: 12843276]
64. Hicks D, Sahel J. The implications of rod-dependent cone survival for basic and clinical research. Invest Ophthalmol Vis Sci. 1999; 40:3071–3074. [PubMed: 10586925]
65. Bird AC. Retinal photoreceptor dystrophies LI. Edward Jackson Memorial Lecture. Am J Ophthalmol. 1995; 119:543–562. [PubMed: 7733180]
66. Raymond SM, Jackson IJ. The retinal pigmented epithelium is required for development and maintenance of the mouse neural retina. Curr Biol. 1995; 5:1286–1295. [PubMed: 8574586]
67. Punzo C, Kornacker K, Cepko CL. Stimulation of the insulin/mTOR pathway delays cone death in a mouse model of retinitis pigmentosa. Nat Neurosci. 2009; 12:44–52. [PubMed: 19060896]
68. Busskamp V, et al. Genetic reactivation of cone photoreceptors restores visual responses in retinitis pigmentosa. Science. 2010; 329:413–417. [PubMed: 20576849]

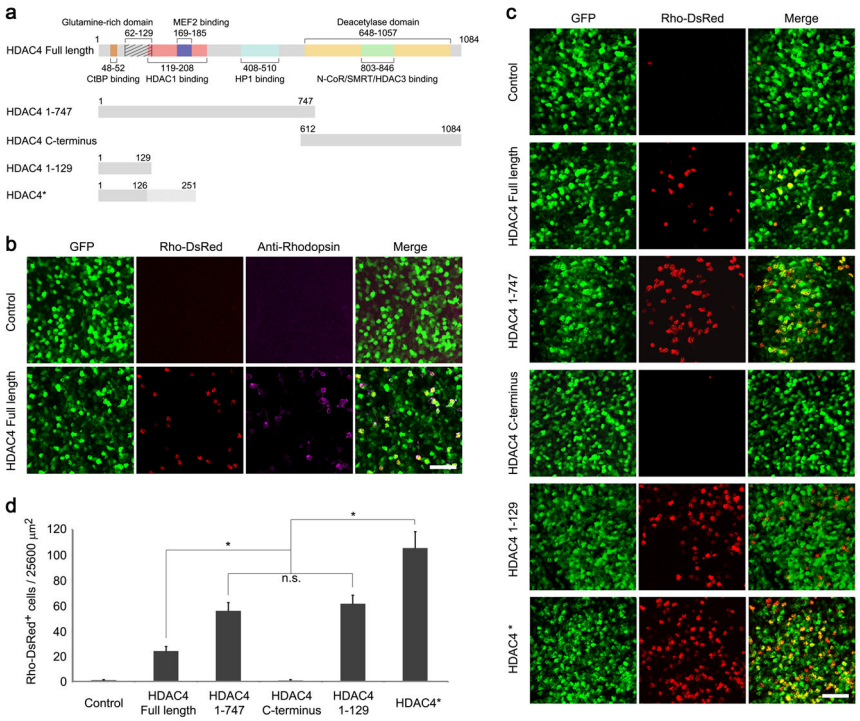

Figure 1.

Preservation of rod photoreceptors by HDAC4 deletion alleles in rd1 mice. (**a**) Schematic representation of HDAC4 functional domains and HDAC4 deletion alleles. (**b**) Co-electroporation of CAG-GFP (transfection marker), CAG-HDAC4 Full Length,, and a rhodopsin reporter construct, Rho-DsRed, in the P0 rd1 retinas with assay at P50 for anti-rhodopsin immunoreactivity. Scale bar, 40 µm. (**c**) Rho-DsRed^{+} rods saved by HDAC4 deletion alleles at P50 in the rd1 retina. Scale bar, 40 µm. (**d**) Quantification of rod survival by HDAC4 Full Length and HDAC4 deletion alleles. Rho-DsRed positive cells were scored per 25600 µm^2 in transfected areas. *P<0.01. Data are presented as mean ± s.d., n=5–8.

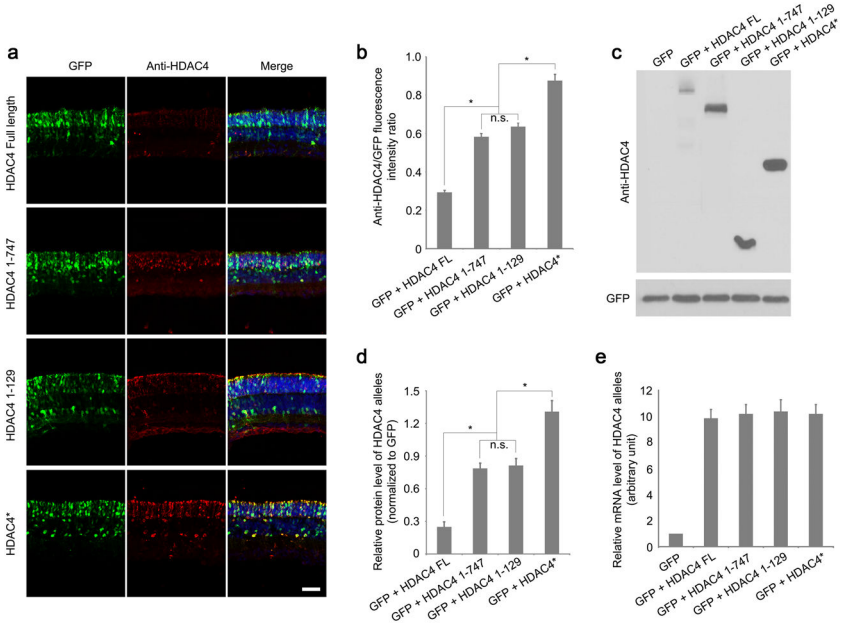

Figure 2.

Protein expression levels of HDAC4 Full Length and HDAC4 deletion alleles. (**a**) Assay of HDAC4 expression using anti-HDAC4 immunohistochemistry in the electroporated rd1 retinas at P12. Scale bar, 40 μm. (**b**) The intensity of anti-HDAC4 immunofluorescence was quantified as a ratio to the fluorescence intensity of co-expressed GFP. **P*<0.01. Data are presented as mean ± s.d., n=3. (**c**) Assay of HDAC4 expression at P12 using anti-HDAC4 western blots in the electroporated rd1 retinas, and quantified (**d**) after normalization to the co-expressed GFP. **P*<0.01. Data are presented as mean ± s.d., n=3. (**e**) Quantitative PCR analysis of mRNA levels of HDAC4 alleles at P12 in the electroporated rd1 retinas. n=3.

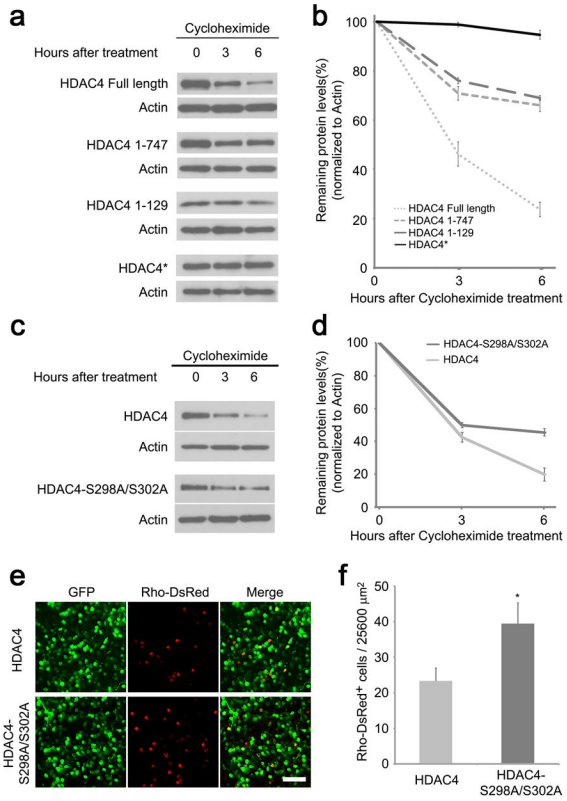

Figure 3.

Enhanced HDAC4 protein stability is correlated with greater rod protection efficiency. (**a**) Protein decay assay of HDAC4 Full Length and deletion alleles. HEK 293T cells were transfected with CAG-HDAC4 or CAG-HDAC4 deletion constructs for 20 hours before treatment with cycloheximide (100μg/ml) for 3 or 6 hours. Cell lysates were immunoblotted for HDAC4. The same immunoblot membranes were stripped and re-probed for actin. (**b**) Protein levels were quantified by densitometry after normalization to actin. Data are presented as mean ± s.d., n=3. (**c**) Protein decay assay for HDAC4 and HDAC4-S298A/S302A mutant. HEK293T cells were transfected with CAG-HDAC4 or CAG-HDAC4-S298A/S302A for 20 hours before treatment with cycloheximide (100μg/ml) for 3 or 6 hours. Cell lysates were immunoblotted for HDAC4. The same immunoblot membranes were stripped and re-probed for actin. (**d**) Protein levels were quantified by densitometry after normalization to actin. Data are presented as mean ± s.d., n=3. (**e**) HDAC4-S298A/S302A saved more rd1 rods in comparison to the wild type HDAC4 at P50. Scale bar, 40 μm. (**f**) Quantification of the preserved rods per 25600 μm^2 on the flat-mount retina. **P*<0.01. Data are presented as mean ± s.d., n=3.

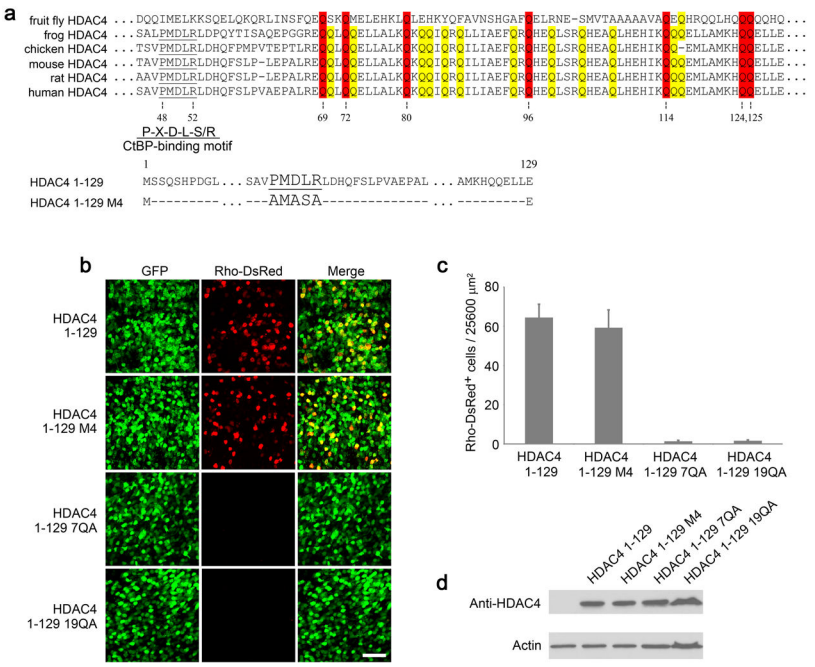

Figure 4.

The conserved glutamines in the HDAC4 N-terminal region are required for rod protection in rd1 mice. (**a**) Cross-species alignment of HDAC4 N-terminal protein sequences reveals conserved glutamine residues, which were mutated to alanines in HDAC4 1-129 19QA (mutated glutamines labeled in red and yellow) and 7QA (mutated glutamines labeled in red). CtBP-binding motif was also mutated in HDAC4 1-129 M4. (**b**) Rod protection by HDAC4 N-terminal mutants in comparison to its wild type form in rd1 mice at P50. Scale bar, 40μm. (**c**) Quantification of the preserved rods per 25600 μm^2 on the flat-mount retina. Data are presented as mean ± s.d., n=6-10. (**d**) Expression of HDAC4 N-terminal mutants was detected by western blots in transfected HEK293T cells.

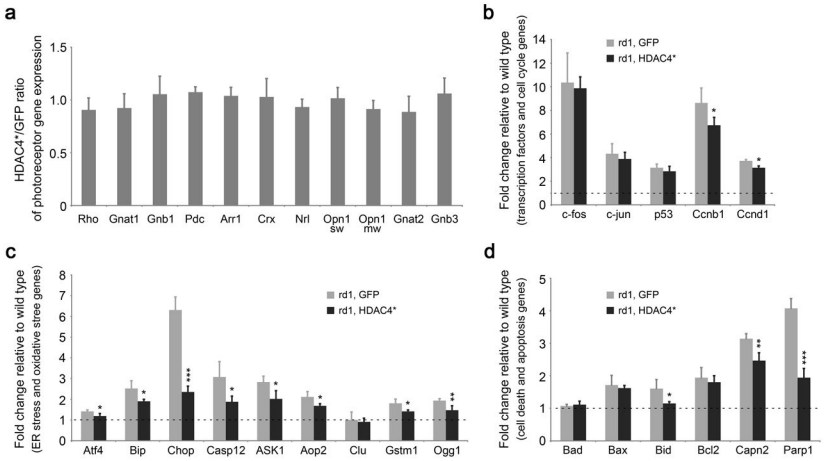

Figure 5.

Profiling gene expression in HDAC4*-electroporated rd1 retinas at P12 by quantitative PCR. (**a**) The mRNA levels of photoreceptor genes in HDAC4*-electroporated rd1 retinas relative to the GFP-electroporated rd1 retinas. (**b**) Assay of gene expression for transcriptional factors and cell cycle genes. (**c**) Assay of gene expression for ER stress and oxidative stress genes. (**d**) Assay of gene expression for cell death/apoptosis genes. Dashed lines in (**b,c,d**) indicate mRNA levels in the wild type retina. **P*<0.05, ***P*<0.01, ****P*<0.001. Data are presented as mean ± s.d., n=3.

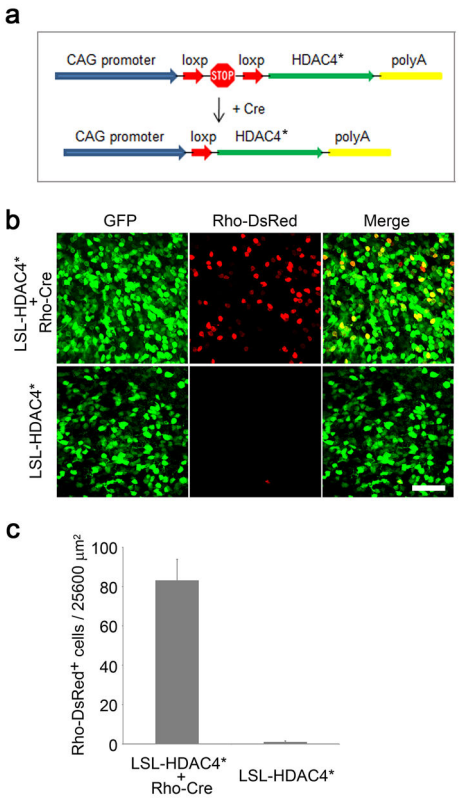

Figure 6.

HDAC4 acts cell-autonomously to protect rd1 rods. (**a**) Schematic illustration of a Cre-responsive expression system to restrict HDAC4 expression in rods. (**b**) Assay of rod survival at P50 in the presence and absence of Rho-Cre. Scale bar, 40 µm. (**c**) Quantification of rod survival per 25600 μm^2 on the flat-mount retina. Data are presented as mean ± s.d., n=3.

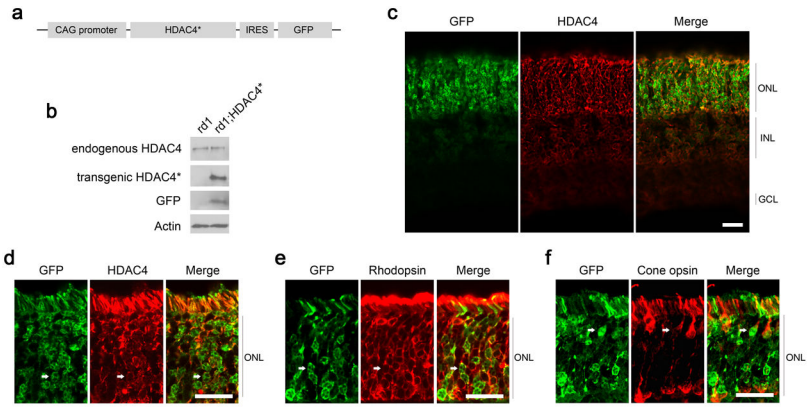

Figure 7.

Construction of HDAC4* transgenic mice. (**a**) Schematic representation of HDAC4* transgenic construct design. (**b**) Immunoblotting analysis of transgene expression in rd1;HDAC4* transgenic mice at P10. (**c–f**) Immunohistochemistry analysis of transgene expression in rd1;HDAC4* transgenic mice at P10 on retinal sections. Scale bar, 20 μm. (**c,d**) Detection of HDAC4 immunoreactivity and the GFP reporter. (**e**) Arrows: transgene expression in rods labeled by anti-rhodopsin immunohistochemistry. (**f**) Arrows: transgene expression in cones labeled by red/green cone opsin immunohistochemistry.

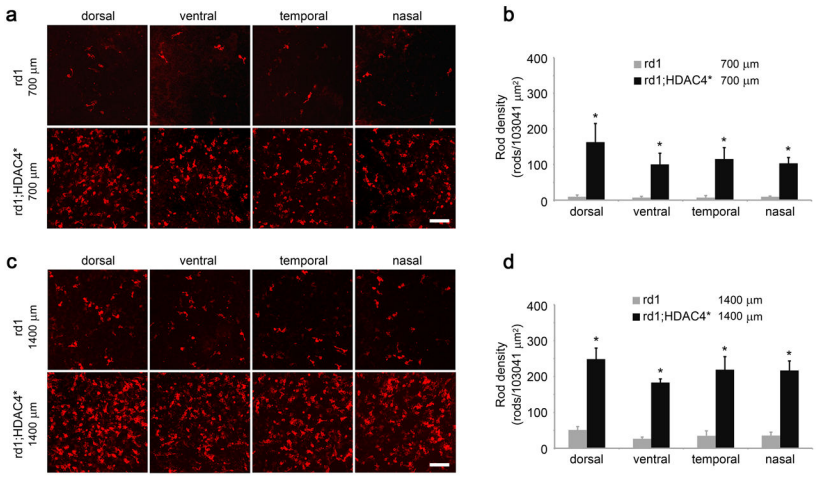

Figure 8.

Prolonged rod survival in HDAC4* transgenic mice. (**a,c**) Detection of rod photoreceptors in HDAC4* transgenic mice and their non-transgenic littermates at P42 by anti-rhodopsin immunohistochemistry on retinal flat mounts at 700 µm (**a**) or 1400 µm (**c**) from the center of the retina. Scale bar, 60 µm. (**b,d**) The number of rods was quantified in the four retinal quadrants (dorsal, ventral, temporal, and nasal) at 700 µm (**b**) or 1400 µm (**d**) from the center of the retina. **P*<0.01. Data are presented as mean ± s.d., n=8.

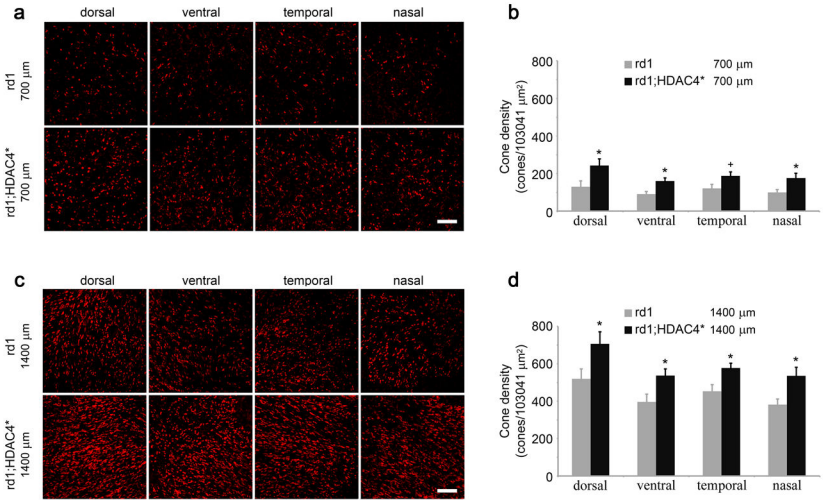

Figure 9.

Prolonged cone survival in HDAC4* transgenic mice. (**a,c**) Detection of cone photoreceptors in HDAC4* transgenic mice and their non-transgenic littermates at P42 by PNA staining on retinal flat mounts at 700 µm (**a**) or 1400 µm (**c**) from the center of the retina. Scale bar, 60 µm. (**b,d**) The density of cones was quantified in the four retinal quadrants (dorsal, ventral, temporal, and nasal) at 700 µm (**b**) or 1400 µm (**d**) from the center of the retina. $^{+}P<0.05$; $^{*}P<0.01$. Data are presented as mean ± s.d., n=8.

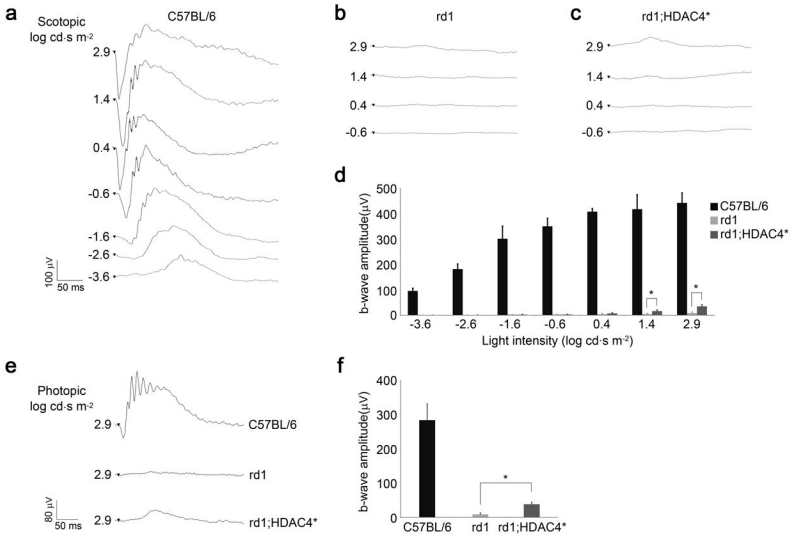

Figure 10.

Measurement of retinal function in HDAC4* transgenic mice. (**a**) Scotopic ERG was recorded at P30 in C57BL/6 wild type retina, (**b**) non-transgenic rd1 retina, and (**c**) rd1;HDAC4* transgenic retina. (**d**) Measured b-wave amplitudes of the scotopic ERG. **P*<0.01. Data are presented as mean ± s.d., n=5-11. (**e**) Photopic ERG was also recorded at P30 in C57BL/6 wild type, rd1;HDAC4* transgenic mice and their non-transgenic rd1 littermates. (**f**) Measured b-wave amplitudes of the photopic ERG. **P*<0.01. Data are presented as mean ± s.d., n=5-11.